News from the Geodesic Acoustic Mode: Magnetic Shear-, q-, and Geometry Effect

K. Hallatschek
Max-Planck-Institut für Plasmaphysik, EURATOM Association, D-85748 Garching, Germany
E-mail: hallatschek@ipp.mpg.de

Abstract. The generation of Geodesic Acoustic Modes (GAM), oscillating poloidal shear flows, has been studied in greater depth by three-dimensional turbulence simulations. A change of the magnetic shear, in particular, a switch to negative shear profoundly affects the amplification mechanism of the GAMs. Negative shear reverses the symmetry of the turbulence modes with respect to the shear flows, altering the sign of the Stringer-Winsor forces. The phenomenon readily suggests an experimental test, which would quantify the role of the Stringer-Winsor effect in comparison to the Reynolds stress in exciting the GAMs. The safety factor q controls the coupling of the GAMs to the parallel velocity, i.e., sound waves. Lowering q increases this coupling. Since the parallel sound waves in turn are heavily damped by the turbulence they act as a loss channel. Thus sufficiently low q cause a quench of the GAM activity, as has been found in recent experiments, too. Finally, the shape of the flux surfaces has great influence on the frequency of the GAMs and the relative strength of the Stringer-Winsor force. Elongation of the plasma column reduces the GAM frequency, and simultaneously increases the energy transfer term due to the up-down asymmetry of the anomalous flux, which can have a dramatic impact on the shear flow level and transport. Again, the results suggest a relatively straightforward comparison with experiments.

1 Introduction

Geodesic Acoustic Modes (GAM), oscillating poloidal shear flows at the characteristic acoustic frequency of a tokamak, are an ubiquitous edge plasma phenomenon in magnetic fusion devices [1,2], and are rapidly gaining attention with progressing experimental detection capabilities [3-5]. The generation of GAMs has been studied in greater depth by three-dimensional turbulence simulations for varying magnetic shear, safety factor, and flux surface geometry.

Thereby the focus has been on the drive mechanisms by either the Reynolds-stress or indirectly by the asymmetric anomalous transport via the Stringer-Winsor-force-term, and on damping by either linear effects or anomalous diffusion of components of the GAM, the pressure perturbations, and the parallel velocity.

GAMs are foremost the rotation of a flux surface about the magnetic axis. Due to the magnetic inhomogeneities and the fact that the magnetic flux is frozen in the plasma, such a motion leads to compression and expansion of individual fluid elements proportional to the change in their ambient B^2. The resulting pressure perturbations are localised predominantly in the upper and lower half of the torus. The free energy [6] necessary to create these pressure perturbations has to come out of the rotation, and the corresponding restoring force term is the Stringer-Winsor-force. (It can also be computed directly from the imbalance in radial magnetic drifts currents due to the up-down asymmetry of the pressure perturbations). Plasma inertia together with the restoring force are all the required ingredients of an oscillator. In a circular tokamak

with concentric flux surfaces, the corresponding oscillations for fluid ions and adiabatic electrons have the frequency $\omega_{\rm GAM} = \sqrt{16/3T/m_i}/R$. Since the regions of opposing pressure perturbations are connected by magnetic field lines, parallel gradients in density and pressure result, which give rise on one hand to parallel sound waves and on the other to parallel dissipation. Both of these depend on the intricacies of the connection by field lines and the flux surface geometry. Moreover, there are also local dissipation mechanisms, such as magnetic pumping, in the edge region of the plasma, where the GAMs are prevalent. The mentioned coupling of sound waves and GAMs makes it sometimes hard to distinguish between the two: A particular mode has the more the character of a GAM, the larger its mean perpendicular kinetic energy is in comparison to the parallel kinetic energy.

The free energy density of the geodesic acoustic mode (assuming adiabatic electrons, singly charged ions and equal electron and ion temperature) may be written as

$$F = \frac{T}{n}\delta n^2 + \frac{1}{\kappa - 1}\frac{n}{2T}\delta T_i^2 + \frac{n m_i v^2}{2}, \tag{1}$$

where $\kappa = 5/3$ is the adiabatic exponent, and n, T are background electron density and temperature, m_i is the ion mass, and v is the fluid ion velocity. Likewise, the free energy input into the geodesic acoustic mode by Reynolds stress, the Stringer-Winsor term, and its reduction by dissipation may be formally written as

$$\partial_t F = 2\frac{T}{n}\delta n'(\tilde{n}\tilde{v}_{E,r}) + \frac{1}{\kappa - 1}\frac{n}{T}\delta T_i'(\tilde{T}_i\tilde{v}_{E,r}) + n m_i v_\perp' R_\perp + n m_i v_\parallel' R_\parallel - \mu F \tag{2}$$

where X' expresses the radial derivative of X, $v_{E,r}$ is the advective radial turbulent $\boldsymbol{E}\times\boldsymbol{B}$-velocity, $R_\perp, R_\parallel$ are the perpendicular and parallel Reynolds stress, and the dissipation rate $-\mu F$ represents the appropriate linear damping of all the components of the GAM. The quadratic quantities $(\tilde{n}\tilde{v}_{E,r}), n/(\kappa-1)(\tilde{T}_i\tilde{v}_{E,r})$ are thus the local turbulent radial flows of particles (Γ) and ion heat (Q).

2 Magnetic Shear

In the literature, the excitation of GAMs is thought to be either caused by Reynolds stress [7] or indirectly by asymmetric anomalous transport enhancing the pressure perturbations associated with the GAM [2,8]. While the former effect is basically independent of the magnetic shear (except to the degree the turbulence itself is susceptible to it), the latter can even change sign and brake it. Numerical experiments varying the magnetic shear – all other paramters identical to reference [2] – have been performed. It turns out that the shear flow (i.e., GAM) level is substantially smaller in the case with negative magnetic shear at $\overline{|v_\theta^2|} = 0.2$ compared to $\overline{|v_\theta^2|} = 0.8$ with positive shear. The overall transport level is in both cases at $Q = 0.23$ owing to the stabilising influence of the negative shear on the turbulence. The decrease is concomitant with a flip in sign of the asymmetric transport drive, whereas the Reynolds stress continues to drive the mode even for negative magnetic shear. Moreover, it is found that the up-down asymmetric transport flips sign in relation to the sign of the shear flow (Fig. 1).

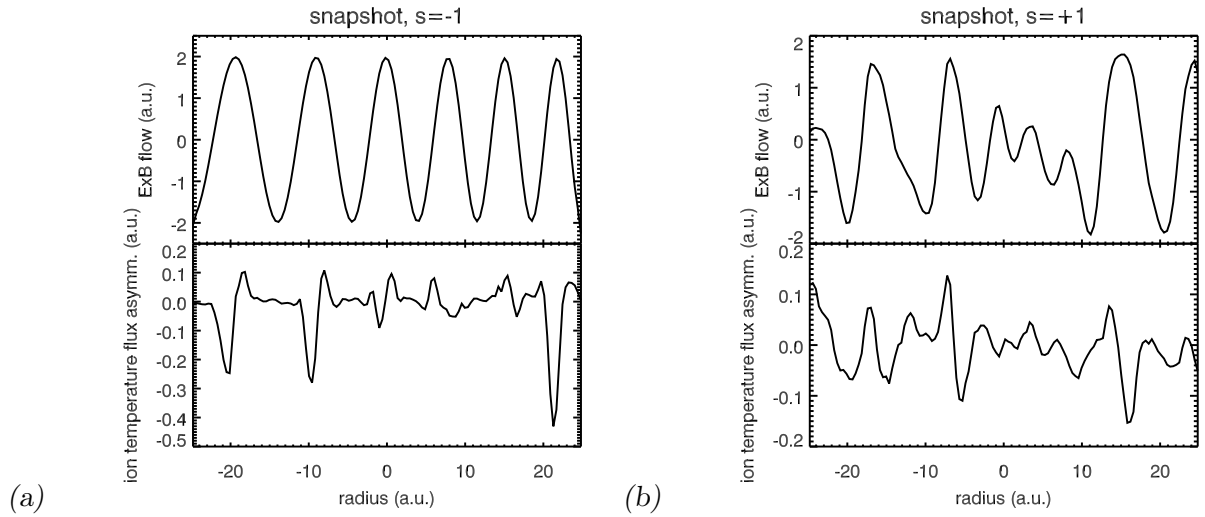

(a) (b)

Fig. 1. Up-down asymmetric component of the turbulent radial heat flux profile $\langle 2/3\tilde{T}v_{E,r}\sin\theta\rangle$ *as function of time in case of negative shear and an artificial flow pattern (a), and positive shear and a self-consistent flow pattern (b). Note the reversed polarity of the transport asymmetry with respect to the local shearing rate*

This effect may be understood in a simple model of the mode structure [8] (which could straightforwardly be generalised to more complex geometry). To good approximation we can assume the electric potential perturbations of a turbulence mode to be field aligned, i.e., a particular wave packet may have the form

$$\delta\phi = A(r,\theta,\phi)\exp(i(k_r + s\theta k_\theta)r + ik_\theta r(\theta - \phi/q)), \tag{3}$$

where A is a slowly varying envelope (typically concentrated near the outboard midplane), r,θ,ϕ are the minor radial, poloidal and toroidal co-ordinate, respectively, k_r, k_θ are the respective wavenumbers at the outboard-midplane (at $\theta = 0$), s is the magnetic shear, and q is the safety factor. Note that all the fast variation is restricted to the exponential factor. After the (growing) GAM has had time to shear the wave packet for a turbulence decorrelation time $\tau_d \ll 1/\omega_{\rm GAM}$, the wavepacket has the form

$$\delta\phi^s = A^s(r,\theta,\phi)\exp(i(k_r + (s\theta - v'_E\tau_d)k_\theta)r + ik_\theta a(\theta - \phi/q)), \tag{4}$$

where for simplicity the shear of the GAM velocity field has been assumed to be constant over the radial extent of the wavepacket. From (4) it is clear that for an originally symmetric mode with $k_r = 0$ at the outboard midplane, the absolute value of the radial wavenumber is now asymmetric about the midplane, depending on the relative signs of magnetic shear (s) and velocity shear (v'_E). To compute the power input into the GAM we consider circular flux surfaces, which result in density and ion temperature fluctuation amplitudes of the form, $\delta n_{\rm GAM} = \delta n_{\rm GAM,0}\sin\theta$, and $\delta T_{\rm GAM} = \delta T_{i,\rm GAM,0}\sin\theta$. For the sake of the argument, let us assume the transport fluxes to be proportional to the turbulence intensity $\delta\phi^2$ by means of proportionality constants γ and q. Then one obtains for the flux surface averaged power density

$$\partial_t\langle F\rangle = \left(2\frac{T}{n}\gamma\delta n'_{\rm GAM,0} + \frac{1}{\kappa - 1}\frac{n}{T}q\delta T'_{i,\rm GAM,0}\right)\langle\sin\theta(A^s)^2(r,\theta,\phi)\rangle, \tag{5}$$

where $\langle\rangle$ indicates the flux surface average, whereby θ varies over all real numbers, as the envelope A^s stems from a ballooning representation. With the other factors independent

of magnetic shear, (except for potential subtle alterations of the turbulence itself), the term determing the GAM-drive is $\langle \sin\theta (A^s)^2(r,\theta,\phi)\rangle$. To exemplify the effect of the mentioned asymmetry of A^s, we take the symmetric mode with $k_r = 0$ at $\theta = 0$, which results in a local radial wavenumber of $k_r(\theta) = (s\theta - v'_E\tau_d)k_\theta$. From drift wave theory it is known that $A^2(1+\rho_s^2(k_r^2+k_\theta^2))$ ($\rho_s \equiv \sqrt{mT}/(eB)$) is an adiabatic invariant, thus we have (for small v'_E):

$$(A^s)^2 = A^2 \frac{1+\rho_s^2(1+(s\theta)^2)k_\theta^2}{1+\rho_s^2(1+(s\theta - v'_E\tau_d)^2)k_\theta^2} \approx A^2\left(1+\frac{2k_\theta^2\rho_s^2}{1+\rho_s^2(1+(s\theta)^2)k_\theta^2} s v'_E \theta \tau_d\right). \qquad (6)$$

With $k_\theta^2\rho_s^2 \ll 1$ the variable asymmetry term from Eq. (5) turns into

$$\langle \sin\theta (A^s)^2(r,\theta,\phi)\rangle = 2\tau_d k_\theta^2\rho_s^2 s v'_E \langle \theta \sin\theta A^2(r,\theta,\phi)\rangle. \qquad (7)$$

For the normal case of strongly ballooned turbulence modes, $\lambda \equiv \langle \theta \sin\theta A^2(r,\theta,\phi)\rangle$ is a positive number of order $\langle A^2\rangle$. The complete average energy transfer is then

$$\overline{\partial_t\langle F\rangle} = 2\tau_d k_\theta^2\rho_s^2 s\lambda\left(2\frac{T}{n}\gamma\overline{\delta n'_{\mathrm{GAM},0}v'_E} + \frac{1}{\kappa-1}\frac{n}{T}q\overline{\delta T'_{i,\mathrm{GAM},0}v'_E}\right), \qquad (8)$$

wherein $\overline{X}$ expresses the time average of X over a GAM oscillation. The density and temperature perturbations lag $\pi/2$ behind the velocity of the GAM. Therefore, the time averages on the right hand side of Eq. (8) nearly vanish except for the fact, that v'_E in Eq. (4) has to be taken a time $\tau_d/2$ in the *past*, since the shearing action is not strictly instantaneously but occurs over a turbulence decorrelation time. Therefore $\overline{\delta n'_{\mathrm{GAM},0}v'_E} \approx \sin(\omega_{\mathrm{GAM}}\tau_d/2)\sqrt{\overline{\delta n'^2_{\mathrm{GAM},0}}\,\overline{v'^2_E}}$, and, with $\sin(\omega_{\mathrm{GAM}}\tau_d/2) \approx \omega_{\mathrm{GAM}}\tau_d/2$,

$$\overline{\partial_t\langle F\rangle} = \omega_{\mathrm{GAM}}\tau_d^2 k_\theta^2\rho_s^2 s\lambda\left(2\frac{T}{n}\gamma\sqrt{\overline{\delta n'^2_{\mathrm{GAM},0}}} + \frac{1}{\kappa-1}\frac{n}{T}q\sqrt{\overline{\delta T'^2_{i,\mathrm{GAM},0}}}\right)\sqrt{\overline{v'^2_E}}. \qquad (9)$$

The sign of this expression is determined by that of the magnetic shear, and a change of it, in particular a switch to negative shear, profoundly affects the amplification mechanism of the GAMs. At positive magnetic shear, the phase of the GAM oscillation with positive flow shear amplifies the turbulence above midplane and reduces it below. When the oscillating flow reaches its turning point, the thus biased turbulence tends to increase the energy stored in the pressure perturbations of the GAM. As a result the flows are growing over an oscillation [6], until higher order effects lead to a saturation. (For the negative-flow-shear phase, the turbulence bias is reversed, as are the pressure perturbations at the turning point. Hence, the effect on the GAM is identical.) Negative magnetic shear reverses the symmetry of the turbulence modes with respect to the shear flows; under otherwise identical circumstances the anomalous transport acts now to brake the GAMs, which results in significantly reduced shear flows. In cases where the GAMs are controlling the turbulent transport level, the effect of negative magnetic shear on the GAMs actually tends to increase the anomalous fluxes. (This action is offset by the well-known stabilising influence of reversed shear on the turbulence itself; whether negative shear is beneficial depends on the balance of the two effects.) The phenomenon suggests an experimental test, where the bias in the turbulence above and below midplane in response to the shear flows is measured. This would quantify the role of the Stringer-Winsor effect in comparison to the Reynolds stress in exciting the GAMs.

3 Safety Factor

Discounting for flux surface shape effects, the safety factor q controls the coupling of the GAMs to the parallel velocity, i.e., sound waves. Lowering q reduces the connection length between the regions of opposing pressure perturbations of the GAM, which increases the parallel pressure gradient, and thus increases this coupling. Since the parallel sound waves in turn are heavily damped by the turbulence – with the parallel velocity basically playing the role of a passive scalar [9] – they act as a loss channel. In general a full Eigenvalue computation is necessary to determine the amount of coupling to the parallel sound waves. However for the case of relatively small coupling, one can set $\rho\partial_t v_\parallel = -\partial_\parallel \tilde{p}$, which yields in Fourier space

$$-i\omega_{\mathrm{GAM}}\rho v_\parallel = -i\tilde{p}/(qR) \Rightarrow v_\parallel = \tilde{p}/(\omega_{\mathrm{GAM}}\rho qR). \tag{10}$$

The parallel flow energy density is therefore

$$F_{v_\parallel} = \frac{\rho v_\parallel^2}{2} = \frac{\tilde{p}^2}{2\rho(\omega_{\mathrm{GAM}}qR)^2}. \tag{11}$$

On the other $\tilde{p} = 2T\tilde{n} + n\tilde{T} = (1+\kappa)T\tilde{n}$, and with Eq. (1) the energy density of the GAM pressure perturbation is $F_p = (1+\kappa)T/(2n)\tilde{n}^2$. The ratio of parallel flow energy to pressure energy is thus for $\kappa = 5/3$ and the above GAM frequency

$$\frac{F_{v_\parallel}}{F_p} = \frac{1}{2q^2}. \tag{12}$$

Similarly, the parallel dissipation due to the parallel temperature gradient is $\partial_t F_T = \nu_\parallel(\kappa-1)^2\tilde{n}^2/((qR)^2)$, where $\nu_\parallel$ is the parallel heat conductivity.

From a collisionless stand point, these arguments have to be taken with the note that now all gradients of even moments of the distribution function cause parallel flows, which are subject to radial turbulent diffusion, and thus dissipation due to phase mixing. In addition, linear Landau-damping due to resonant particles becomes possible for low enough q [10]. Therefore, sufficiently low q cause a quench of the GAM activity, as has been found in recent experiments [11], too.

The following table shows the effects of reducing q from 4 to 1 in turbulence simulations again with the other parameters taken from the core-edge transitional regime in ref. [2].

$q = 4$	$q = 1$ (for $v_\parallel$ only)	$q = 1$ (for $v_\parallel$ and $q_\parallel$ only)
$\overline{\lvert v_\theta^2\rvert} = 0.83$	$\overline{\lvert v_\theta^2\rvert} = 0.67$	$\overline{\lvert v_\theta^2\rvert} = 0.46$
$\overline{\lvert v_\parallel^2\rvert} = 0.06$	$\overline{\lvert v_\parallel^2\rvert} = 0.45$	$\overline{\lvert v_\parallel^2\rvert} = 0.18$

It shows clearly that the parallel velocity component dramatically increases with decreasing connection length, while the GAM amplitude decreases without quenching completely. It must be born in mind, however, that the experimental results [11] were obtained in shaped discharges, which add significant complexity, as is detailed below.

4 Flux Surface Shape

Shape and local radial separation of the flux surfaces has great influence on the frequency of the GAMs and the relative strength of the Stringer-Winsor force, i.e., the relative

importance of pressure fluctuations and poloidal flow. The flux surface separation changes the local poloidal velocity by means of

$$v_{E,\theta} \propto E_r = \frac{\mathrm{d}\phi}{\mathrm{d}\psi}|\nabla\psi|, \tag{13}$$

where ψ is the flux surface label. The (major) radial velocity is

$$v_{E,R} \propto E_z = \frac{\mathrm{d}\phi}{\mathrm{d}\psi}|\partial_z\psi|, \tag{14}$$

where z is the vertical co-ordinate. For example, an elongation of the plasma column leads to a larger distance between flux surfaces away from the midplane, reducing the radial electric field of the GAM there relative to the outboard midplane. Nevertheless the velocity at the outboard midplane is the quantity relevant to the modulation or shearing of the turbulence. This leads to a reduction of the radial excursion and thus lower pressure fluctuations associated with a fixed poloidal flow amplitude given at the outboard midplane. Lowering the pressure fluctuations also reduces the Stringer-Winsor force during the GAM oscillation, resulting in a reduced frequency compared to a circular plasma column.

Discarding for simplicity the temperature fluctuations, one can write an effective GAM system for large aspect ratio R/a as

$$\partial_t n_s = \sqrt{2} n C_1 \frac{v_0}{R}, \tag{15}$$

$$\rho C_2 \partial_t v_0 = -2\sqrt{2} T C_1 \frac{n_s}{R}, \tag{16}$$

where

$$n_s \equiv \frac{\langle \tilde{n}\partial_z\psi\rangle}{\sqrt{\langle(\partial_z\psi)^2\rangle}} \tag{17}$$

is the amplitude of the density perturbations and v_0 is the poloidal velocity at the outboard midplane. The effective equations are controlled by two coefficients describing the compression for a given poloidal velocity v_0,

$$C_1 \equiv \frac{\sqrt{2\langle(\partial_z\psi)^2\rangle}}{|\nabla\psi(\theta=0)|}, \tag{18}$$

and the effective inertia of the flow,

$$C_2 \equiv \frac{\langle(\nabla\psi)^2\rangle}{|\nabla\psi(\theta=0)|^2}, \tag{19}$$

whose definitions are such that for circular geometry $C_1 = C_2 = 1$.

From (15,16) one obtains the modified GAM frequency

$$\omega_{\mathrm{GAM}} = 2C_1/\sqrt{C_2}\frac{1}{R}\sqrt{\frac{T}{m_i}}. \tag{20}$$

Assuming that the combined drive terms due to Reynolds stress and asymmetric anomalous transport have a limit in terms of the achievable pressure (here density) perturbation n_s, the poloidal velocity is determined by

$$v_0^2 = \frac{2T}{\rho n C_2} n_s^2. \tag{21}$$

For a Miller equilibrium [12], it can be shown that for increasing elongation $\kappa \to \infty$ or differential Shafranov shift $\mathrm{d}R/\mathrm{d}r \to -1$ all C_1, C_2 and likewise ω_{GAM} tend towards zero.

Further complications arise, if the interaction with the parallel sound waves is taken into account, as on non-circular or shifted flux surfaces pressure perturbations other than $m = 1$ can be exited. These have higher resonance frequencies, which even for edge parameters can be resonant with the GAM, and have much reduced connection length which enhances damping of the GAMs as discussed in the previous section.

To demonstrate the importance of flux surface shaping (in the absence of the mentioned complications), figure 2 displays the oscillating shear flow patterns, and the transport from two turbulence simulation runs with the GAM pressure perturbations reduced (a,c) or increased (b,d) by a factor two in comparison to the flow velocity, corresponding to an ellipticity of 2.5 and 0.66, respectively, at otherwise constant turbulence conditions.

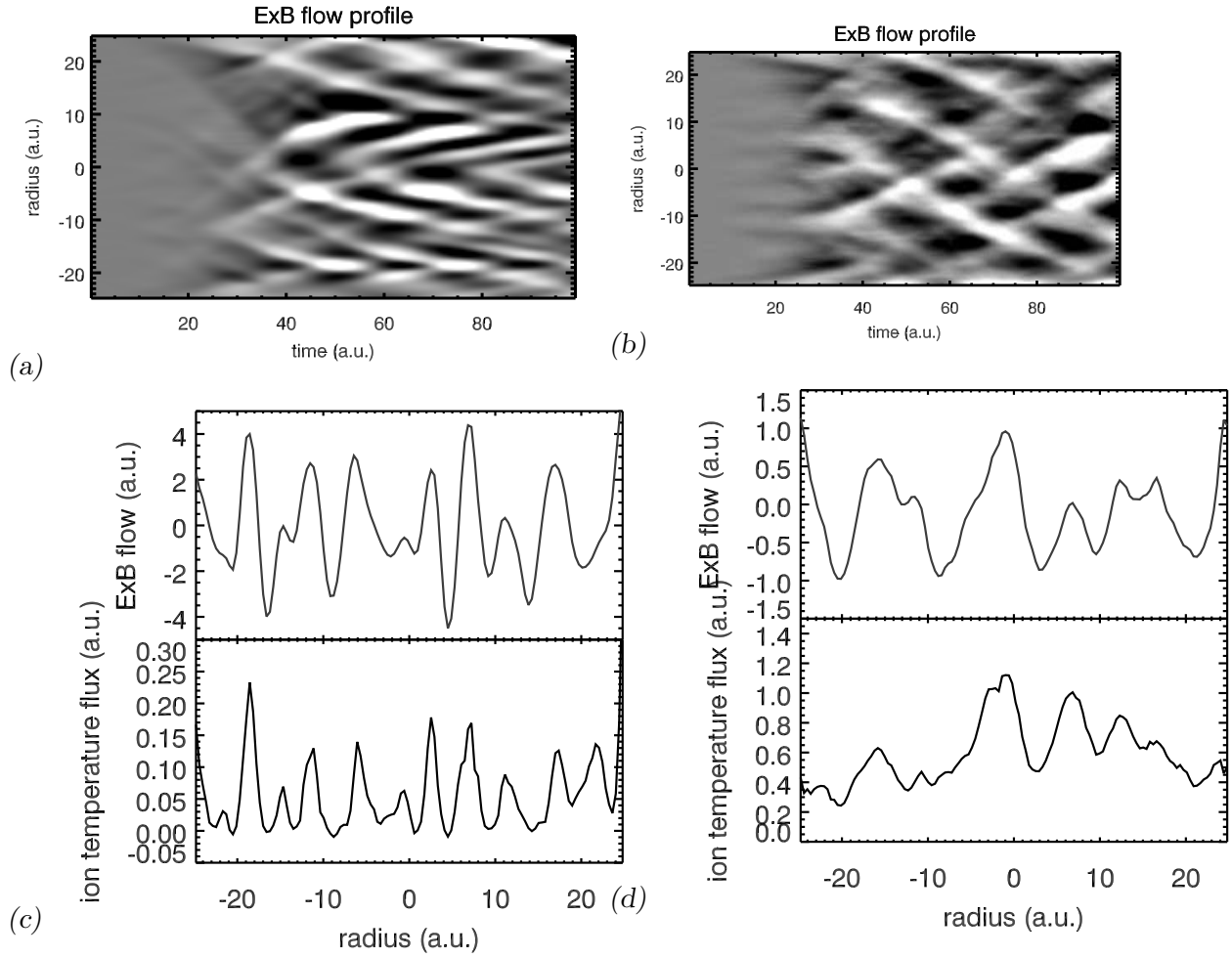

Fig. 2. Anomalous radial heat flux profile as function of time in case of favourable (a) and unfavourable (b) flux surface geometry; (c) and (d) show snapshots of poloidal $\boldsymbol{E} \times \boldsymbol{B}$-flow and radial heat flux at $t = 80$ corresponding to (a) and (b), respectively. The strong correlation between flows and radial heat flux is well understood [2].

The plasma parameters for the turbulence were in the transitional regime between core and edge (drift parameter $\alpha_d = 0.6$, $\epsilon_n = L_n/(2R) = 0.08$, $q = 3.14$, $\hat{s} = 1$, $\eta_i = 3$, [2]). The dramatic difference in transport of about one order of magnitude demonstrates that optimisation of the magnetic geometry with respect to the GAMs (in contrast to the turbulence alone) is likely another tempting route to improved confinement. Again, the

results suggest a relatively straightforward comparison with experiments.

[1] N. Winsor, et al., Phys. Fluids **11**, *2448 (1968)*
[2] K. Hallatschek, D. Biskamp, Phys. Rev. Lett. **86**, *1223 (2001)*
[3] G. R. McKee, R.J. Fonck, M. Jakubowski et al., Phys. Plasmas **5**, *1712 (2003)*
[4] A. Fujisawa, K. Itoh, et al., Phys. Rev. Lett **93**, *165002 (2004)*
[5] G. D. Conway, B. Scott, et al., Plasma Phys. Control. Fusion **47**, *1165 (2005)*
[6] K. Hallatschek, Phys. Rev. Lett. **93**, *1250001 (2004)*
[7] P.H. Diamond, S.-I. Itoh, K. Itoh, T.S. Hahm, Plasma Phys. Control. Fusion **47**, *R35 (2005)*
[8] K. Itoh, K. Hallatschek, et al., Plasma Phys. Control. Fusion **47**, *451 (2005)*
[9] K. Hallatschek, Phys. Rev. Lett. **93**, *65001 (2004)*
[10] F.L. Hinton, M.N. Rosenbluth, Plasma Phys. Control. Fusion **41**, *A653 (1999)*
[11] G.R. McKee, et al., Plasma Phys. Control. Fusion **48**, *S123 (2006)*
[12] R.L. Miller, et al., Phys. Plasmas **5**, *973 (1998)*